

Atomic-scale characterization of the CdS/CuInSe₂ interface in thin-film solar cells

O. Cojocaru-Mirédin,^{1,a)} P. Choi,¹ R. Wuerz,² and D. Raabe¹

¹Max-Planck-Institut für Eisenforschung, Max-Planck-Str. 1, 40237 Düsseldorf, Germany

²Zentrum für Sonnenenergie-und Wasserstoff-Forschung Baden-Württemberg, Industriestr. 6, 70565 Stuttgart, Germany

(Received 19 October 2010; accepted 5 February 2011; published online 8 March 2011)

Elemental mixing at the CdS/CuInSe₂ interface of a thin-film solar cell was studied by means of atom probe tomography. A Cu-depleted and Cd-doped region (~ 2 nm in width) was detected at the CuInSe₂ surface, proving the existence of a buried p-n homojunction within the CuInSe₂ absorber layer. Furthermore, CdS was found to infiltrate open pores existing in CuInSe₂ during the chemical bath deposition. This could explain why chemical bath deposition of CdS leads to higher solar cell efficiencies compared to physical vapor deposition of CdS. © 2011 American Institute of Physics. [doi:10.1063/1.3560308]

Thin-film solar cells based on CuInSe₂ (CIS) [and its derivative Cu(In,Ga)Se₂ (CIGS)] have been under development for more than 30 years because of their high efficiency, long-term stability, and low-cost production.¹⁻³ Optimized deposition and processing steps for the constituent layers have led to date to maximum energy conversion efficiencies of 20.3% for CIGS solar cells.⁴ Thus, CIGS-based solar cells belong to the most promising candidates for large-scale photovoltaic energy conversion.

Despite the outstanding performance of these solar cells, the separation mechanisms for photogenerated charge carriers at the CdS/CI(G)S p-n junction remain far from being understood. This is mainly due to a lack of information on local chemical changes across the CdS/CI(G)S interface, in particular, at the atomic scale.

Previous studies on the interface between CdS buffer layers and CI(G)S absorber layers relied on spectroscopic methods such as energy dispersive x-ray spectroscopy (EDX),^{5,6} x-ray emission spectroscopy,⁷ x-ray photoelectron spectroscopy,^{7,8} Auger electron spectroscopy,⁸ and secondary ion mass spectrometry (SIMS).⁸ Using these techniques the buffer/absorber layer interface was found to be intermixed, suggesting that the idea of an abrupt p-n heterojunction, as commonly assumed in device simulations,⁹ is incorrect when modeling the characteristics of CI(G)S solar cells. Furthermore, the existence of a buried homojunction within the absorber layer was proposed, based on the detection of a Cd-doped surface zone in CI(G)S,^{5,6,8} and confirmed by scanning Kelvin probe microscopy studies.¹⁰

Although the above-mentioned techniques have been successfully applied to the characterization of the CdS/CI(G)S interface, they do not provide sufficiently high spatial resolution and accurate compositional data for a complete understanding of the p-n junction. Spatially resolved chemical analyses below the nanoscale are needed to understand the junction formation in CIS-based solar cells and its effect on the energy conversion efficiency.

This letter presents for the first time three-dimensional data on the elemental distribution across CdS/CIS interfaces obtained by atom probe tomography (APT). APT, a combi-

nation of time of flight mass spectrometry and ion projection microscopy,¹¹ allows three-dimensional elemental mapping with near-atomic resolution and high detection sensitivity, thus enabling highly accurate chemical analyses of buried interfaces.

The solar cell studied in this work was fabricated by co-evaporation of a polycrystalline CuInSe₂ film onto a Mo-coated soda lime glass substrate in a single-stage inline process at about 600 °C.¹² The CdS layer was deposited by chemical bath deposition (CBD). In this process CdSO₄, ammonia and thiourea were mixed and a ~ 60 nm thick CdS film was grown in 10 min at 65 °C. An intrinsic ZnO layer and a ZnO:Al front contact layer was finally deposited by rf and dc sputtering, respectively.

Cross-sectional analyses of the solar cell were done using transmission electron microscopy (TEM) (JEOL 2200 FS at 200 kV). APT experiments were performed with a local electrode atom probe (LEAPTM 3000X HR, Cameca Instruments), applying laser pulses of 532 nm wavelength, 12 ps pulse length, and an energy of 0.1 nJ per pulse at a repetition rate of 100 kHz. The specimen base temperature was about 60 K. Both TEM and APT samples were prepared using a dual beam focused-ion-beam (FEI Helios Nanolab 600), where APT samples were prepared according to the procedure described in Refs. 13 and 14. To minimize beam damage, a low energy (5 keV) Ga beam was used at the final ion-milling stage.

Figure 1 shows the cross-sectional bright field TEM image of the ZnO, CdS, and CIS layers. In contrast to the relatively large grains of the CIS layer (~ 0.7 to 1.25 μm), the CdS layer consists of very small grains (~ 10 to 15 nm). Although the CIS layer exhibits substantial surface roughness (~ 120 nm in average), the CdS layer grown on top of CIS has a uniform thickness (~ 60 nm). Top-view scanning electron microscope images of this CIS layer, taken after removing the CdS and ZnO layers by chemical etching, revealed a large number of open pores inside the absorber material (not shown).

Figure 2(a) shows a three-dimensional elemental map which contains the CdS/CIS interface, tilted with respect to the direction of analysis. The detection of a tilted interface is not surprising when taking into account the interfacial rough-

^{a)}Electronic mail: o.cojocaru-miredin@mpie.de.

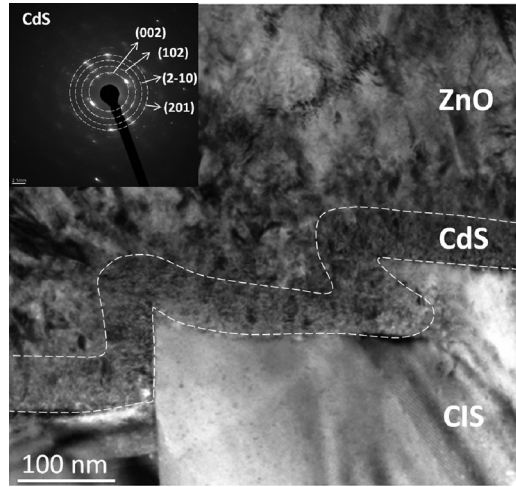


FIG. 1. Bright-field TEM image of the CIS/CdS/ZnO interfaces. The CdS layer as identified by a selected area diffraction pattern (see inset) has uniform thickness (~ 60 nm).

ness observed by TEM (see Fig. 1). For a quantitative analysis, a concentration profile across the CdS/CIS interface [see Fig. 2(b)] was plotted as a proximity histogram (for details see Ref. 15). An isoconcentration surface of 26 at. % Cd was defined as the interface. It can be seen in Fig. 2(b) that the CdS/CIS interface is rather diffuse (~ 2 nm width). Close to the CIS surface there is a distinct zone of about 2 nm in width [marked in gray in Fig. 2(b)] in which the Cu concentration decreases while the In and Se concentrations remain constant. In this region, an increased Cd concentration can be detected as opposed to S, which remains essentially unchanged. The dashed areas in Fig. 2(b) give the number density of the “missing” Cu ions and surplus Cd ions close to the CIS surface. These yield nearly the same values ($1.65 \times 10^{22} \text{ cm}^{-3}$ and $1.7 \times 10^{22} \text{ cm}^{-3}$, respectively) showing that Cu vacancies at the CIS surface are occupied by Cd atoms. The observed replacement of Cu by Cd is in good agreement with previous results obtained by EDX (Refs. 5 and 6) and SIMS.⁸ Figure 2(b) also shows that Cu, In, and Se atoms have diffused into the CdS layer during the processing of the solar cell. It is worth noting that the Cu depletion in the CIS layer could not only be due to the diffusion from the CIS into CdS but also partly due to Cu dissolution in the chemical bath. The average composition of the CIS layer determined from the composition profile (23.3 at. % Cu, 29 at. % In, 46.7 at. % Se) is in good agreement with x-ray fluorescence spectroscopy measurements for the integral composition (21.4 at. % Cu, 27.8 at. % In, and 50.8 at. % Se). The lower concentration value of Se and higher values of Cu and In measured by APT may be ascribed to preferential field evaporation of Se atoms between the laser pulses. The average CdS composition determined from the concen-

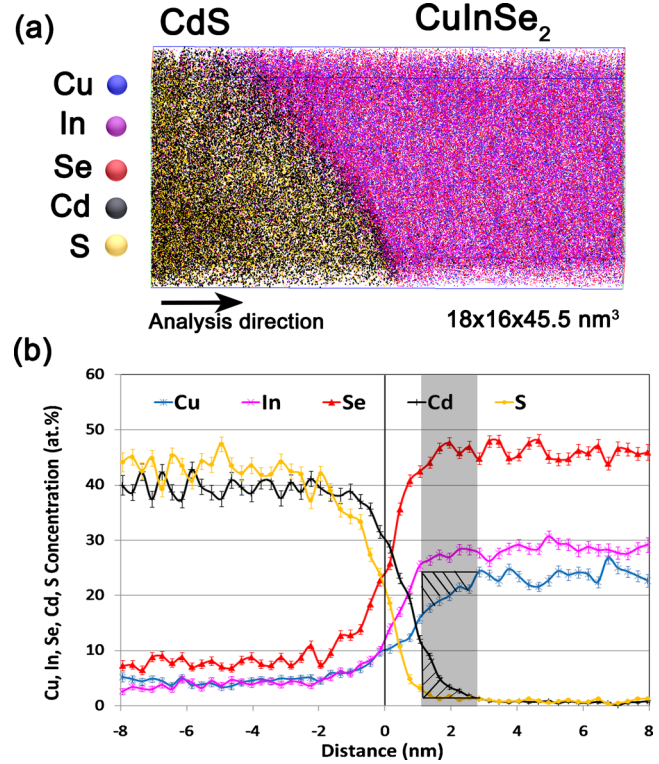


FIG. 2. (Color online) (a) APT elemental maps of Cu, In, Se, Cd, and S. The volume size shown is $18.5 \times 16 \times 45.5 \text{ nm}^3$. (b) Proximity histogram with respect to the Cd 26 at. % isoconcentration surface and 0.3 nm bin size.

tration profile exhibits a significant deviation from the nominal 50:50 stoichiometry [see Fig. 2(b)]. This is due to some overlapping mass-to-charge peaks ($^{113}\text{Cd}^+$ and $^{113}\text{In}^+$, $^{140,142,147}\text{CdS}^+$ and $^{140,142,147}\text{CuSe}^+$), which cannot be deconvoluted in the composition profile and lead to an overestimation of the In, Cu, and Se concentration in CdS. To determine a more accurate value for the actual composition of the CdS layer, the mass spectrum of the CdS layer was evaluated separately. Overlapping mass peaks were deconvoluted into the possible elements or compounds by taking into account the isotope abundances. The values corrected by this procedure are shown for both CdS and CIS in Table I. The sum of the cation (Cd, Cu, and In) and anion (S, Se) concentrations nearly yields the expected 50:50 stoichiometry, indicating that Cd is partly substituted by Cu and In, while S is partly substituted by Se. The existence of an ordered defect compound as proposed by Schmid *et al.*¹⁶ can be excluded by the APT concentration profile in [Fig. 2(b)] at least for this sample.

Figure 3(a) shows the result of an APT analysis in which CdS could be detected inside the CIS absorber layer more than 100 nm below the surface. A closer view from different directions shows that the detected CdS zone is platelike and

TABLE I. Chemical composition values of CdS and CuInSe₂ layers obtained from APT mass-to-charge spectra after deconvolution of overlapping mass peaks.

Analysis	Layer	Cu (at. %)	In (at. %)	Se (at. %)	Cd (at. %)	S (at. %)
APT-1 Figure 2	CdS	2.90 ± 0.05	0.93 ± 0.02	1.00 ± 0.02	46.00 ± 0.08	48.70 ± 0.08
	CIS	22.00 ± 0.06	29.00 ± 0.07	48.00 ± 0.08	0	0
APT-2 Figure 3	CdS	4.70 ± 0.05	4.00 ± 0.05	1.80 ± 0.03	41.50 ± 0.08	47.30 ± 0.08
	CIS	22.50 ± 0.06	28.30 ± 0.07	48.80 ± 0.08	0	0

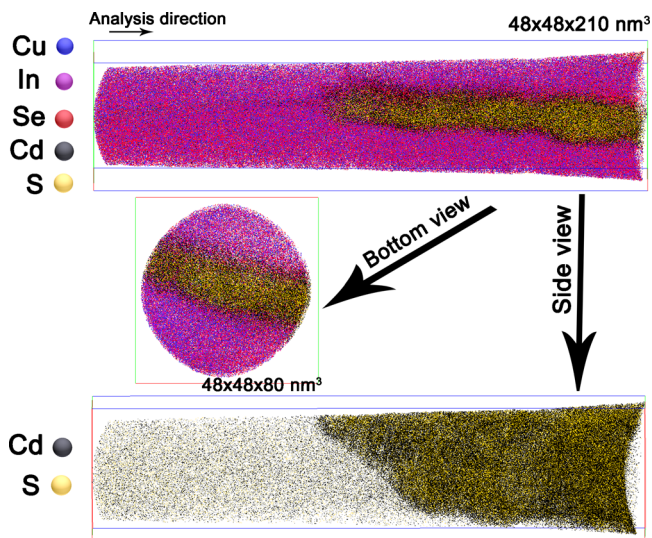


FIG. 3. (Color online) APT elemental maps of Cu, In, Se, Cd, and S, in three different views. The volume size shown here is $48 \times 48 \times 210 \text{ nm}^3$.

not completely enclosed by CIS in the analyzed volume. The existence of the CdS phase beneath the CIS layer can be explained by the infiltration of open pores in CIS during the CBD. The bulk composition values of CdS and CIS, obtained after the deconvolution of overlapping mass peaks, are shown in Table I. Cu, In, and Se concentrations in CdS are higher than for the first measurement. This may be because the CdS zone shown in Fig. 3(a) has a plate-like shape and is enclosed by CIS. Cu, In, and Se atoms can diffuse into CdS from different directions, resulting in higher solute concentrations.

The main results of our APT analyses on the CdS/CIS interface can be summed up as follows: (i) Cu, In, and Se atoms exist in the CdS layer. This can be explained by diffusion phenomena, (ii) Cu vacancies at the CIS surface are occupied by Cd, and (iii) open pores in CIS are infiltrated with CdS during the CBD.

APT reveals, in good qualitative agreement with previous EDX studies but near atomic scale resolution,^{5,6} a Cd-doped surface region of the absorber layer. The bivalent Cd ions are expected to act as substitutional donors on monovalent Cu sites due to the similar ionic radii of Cd^{2+} (0.097 nm) and Cu^+ (0.096 nm).⁵

The maximum dopant density estimated from our composition profiles is on the order of 10^{22} cm^{-3} , clearly exceeding typical hole density values in solar grade CIS layers ($p = 2 \times 10^{15} \text{ cm}^{-3}$).¹⁷ Thus, we conclude that the Cd-doped CIS surface layer is inverted from p-to n-type, and a buried, shallow p-n homojunction is formed instead of a heterojunction between CdS and CIS. The homojunction formation is expected to improve the efficiency of the solar cell due to a

reduction in interfacial recombination of charge carriers.¹⁸ Our studies also have shown that open pores inside CIS can be filled with CdS by the CBD process. Open pores inhibit charge carrier transport, and therefore, their infiltration with CdS is beneficial. This could explain why the efficiency of the solar cells with a CBD-CdS buffer layer is much higher compared to cells with a CdS buffer layer deposited by physical vapor deposition.⁶

Finally, it should be noted that the observations and conclusions made in this work for this particular sample cannot be generally transferred to all CI(G)S solar cells. Different absorber compositions and deposition methods may well result in different chemical gradients across the p-n junction. Nevertheless, this work shows that APT in combination with efficiency data is a highly promising technique for elucidating the relationship between compositional variations across the p-n junction and cell efficiency.

The authors would like to thank Wolfram Witte and Aleksander Kostka for their help in this work.

¹B. J. Stanbery, *Crit. Rev. Solid State Mater. Sci.* **27**, 73 (2002).

²M. Kemell, M. Ritala, and M. Leskelä, *Crit. Rev. Solid State Mater. Sci.* **30**, 1 (2005).

³L. L. Kazmerski, *J. Electron Spectrosc.* **150**, 105 (2006).

⁴P. Jackson, M. Powalla, E. Lotter, D. Hariskos, S. Paetel, R. Wuerz, R. Menner, and W. Wischmann, "New world record efficiency for Cu(In,Ga)Se₂ solar cells beyond 20%," *Prog. Photovoltaics* (to be published) (2011).

⁵T. Nakada and A. Kunioka, *Appl. Phys. Lett.* **74**, 2444 (1999).

⁶D. Abou-Ras, G. Korstörz, A. Romeo, D. Rudmann, and A. N. Tiwari, *Thin Solid Films* **480–481**, 118 (2005).

⁷C. Heske, D. Eich, R. Fink, E. Umbach, T. van Buuren, C. Bostedt, L. J. Terminello, S. Kakar, M. M. Grush, T. A. Callcott, F. J. Himpsel, D. L. Ederer, R. C. C. Perera, W. Riedl, and F. Karg, *Appl. Phys. Lett.* **74**, 1451 (1999).

⁸D. Liao and A. Rockett, *J. Appl. Phys.* **93**, 9380 (2003).

⁹R. Klenk, *Thin Solid Films* **387**, 135 (2001).

¹⁰C. S. Jiang, F. S. Hasoon, H. R. Moutinho, H. A. Al-Thani, M. J. Romero, and M. M. Al-Jassim, *Appl. Phys. Lett.* **82**, 127 (2003).

¹¹M. K. Miller, A. Cerezo, and M. G. Hetherington, *Atom Probe Field Ion Microscopy* (Clarendon, WIP Munich, 1996).

¹²M. Powalla, G. Voorwinden, and B. Dimmler, in *Proceedings of the 14th European Photovoltaic Solar Energy Conference*, edited by H. A. Ossensbrink, P. Helm, and H. Ehmann, Barcelona, Spain, 30 June–4 July, 1997, p. 1270.

¹³M. K. Miller, K. F. Russell, K. Thompson, R. Alvis, and D. J. Larson, *Microsc. Microanal.* **13**, 428 (2007).

¹⁴K. Thompson, D. Lawrence, D. J. Larson, J. D. Olson, T. F. Kelly, and B. Gorman, *Ultramicroscopy* **107**, 131 (2007).

¹⁵O. C. Hellman, J. A. Vandenbroucke, J. Rusing, D. Isheim, and D. N. Seidman, *Microsc. Microanal.* **6**, 437 (2000).

¹⁶D. Schmid, M. Ruckh, F. Grunwald, and H. W. Schock, *J. Appl. Phys.* **73**, 2902 (1993).

¹⁷T. Eisenbarth, T. Unold, R. Caballero, C. A. Kaufmann, and H. W. Schock, *J. Appl. Phys.* **107**, 034509 (2010).

¹⁸N. H. Quang, "The role of the heterointerfaces in the Cu(In,Ga)Se₂ thin film solar cell with chemical bath deposited buffer layers," Ph.D. thesis, Stuttgart University, 2004.